Catal Lett (2014) 144:2114–2120
DOI 10.1007/s10562-014-1384-4

On the Temperature Programmed Desorption of Hydrogen from Polycrystalline Copper

Matthias B. Fichtl · Olaf Hinrichsen

Received: 7 August 2014 / Accepted: 30 September 2014 / Published online: 17 October 2014

Abstract Temperature programmed hydrogen desorption (H_2-TPD) is a versatile tool to characterize metal surfaces in heterogeneous catalysts. We present a systematic H_2-TPD study combined with a kinetic analysis of the H_2 desorption process from pure polycrystalline copper and alumina supported copper. The results show that, in contrast to typical Cu/ZnO based methanol synthesis catalysts, the alumina support has no measureable influence on the desorption process and that the copper surface in both catalyst can be accurately described by a theoretically deduced mixture of the low index planes Cu(100), Cu(110), and Cu(111).

Key words Heterogeneous catalysis · Catalysis · Elementary kinetics · Copper catalysts

List of Symbols

η_{hkl}	Resulting facet fraction (–)
σ_{hkl}	Copper surface atom density (mol m^{-2})
N_{H_2}	Specific hydrogen adsorption capacity on the catalyst (mol g_{cat}^{-1})
$N_{H_2,hkl}$	Specific hydrogen adsorption capacity on facet hkl (mol g_{cat}^{-1})
$\Theta_{H,hkl}$	Hydrogen coverage on facet hkl (–)
n_{H_2}	Molar amount of hydrogen (mol)
$\dot{n}_{H_2}$	Molar flux of hydrogen (mol s^{-1})
$\dot{n}_{H_2,0}$	Molar flux of hydrogen at the reactor inlet (mol s^{-1})
T	Temperature (K)
$E_{A,hkl}$	Activation energy of H_2 desorption from facet hkl (kJ mol^{-1})
E_{Θ}	Difference in activation energy of H_2 desorption due to a full covered surface (kJ mol^{-1})
$k_{o,hkl}$	Prefactor of H_2 desorption from facet hkl (s^{-1})
R	Ideal gas constant (J mol^{-1} K^{-1})
n	Order of coverage dependency (–)
m_{calc}	Mass of calcined catalyst (kg^{-1})

1 Introduction

In order to understand the activity and nature of supported metal catalysts, the characterization of the metal surface exposed to the gas atmosphere during reaction conditions is of vital importance. Typically, this is done by specific chemisorption of a probe molecule like hydrogen or carbon monoxide on the metal followed by quantification of the adsorbed amount either by frontal chromatography, pressure or concentration programmed techniques or temperature programmed desorption (TPD).

In case of copper based methanol synthesis catalysts two major techniques, the reactive N_2O frontal chromatography (N_2O-RFC) and temperature programmed hydrogen desorption (H_2-TPD), have been developed to analyze catalyst activity behavior [1, 2]. Especially the N_2O-RFC is widely employed due to its simplicity and fast measuring process. Although recent results showed

---

Electronic supplementary material The online version of this article (doi:10.1007/s10562-014-1384-4) contains supplementary material, which is available to authorized users.

M. B. Fichtl · O. Hinrichsen (✉)
Chemistry Department, Technische Universität München,
Lichtenbergstraße 4, 85748 Garching bei München, Germany
e-mail: olaf.hinrichsen@ch.tum.de

M. B. Fichtl · O. Hinrichsen
Catalysis Research Center, Technische Universität München,
Ernst-Otto-Fischer-Straße 1, 85748 Garching bei München,
Germany

that the application of N_2O-RFC in typical $Cu/ZnO/Al_2O_3$ systems does not only oxidize the copper surface, but also oxygen defect sites generated at the Cu/ZnO interface, a linear relationship between activity and N_2O adsorption capacity can often be established for catalysts with similar preparation history [3–5]. In contrast, the H_2-TPD method only describes the exposed copper surface area, but suffers from a more challenging experimental effort as the dissociative adsorption of hydrogen on copper is an activated process and full coverage is only achieved at low temperatures using elevated pressure or predecomposed atomic hydrogen [6, 7]. Apart from a pure quantification of the exposed metal surface area, the desorption signal also contains useful information about the hydrogen desorption enthalpy or possible metal-support interactions in the catalyst. As shown for $Cu/ZnO/Al_2O_3$ systems, this technique enables to monitor dynamic morphologic changes of the copper crystallites which are induced by partial reduction of the ZnO in vicinity to copper [8–10]. As this process is a function of the gas atmosphere reduction potential and influences the catalyst activity it has also been included in a microkinetic model which can be extrapolated to industrially relevant conditions [11–13]. However, the nature of the copper surface probed by H_2 desorption is still vague. On the one hand, the activity of typical copper based methanol synthesis catalysts is definitely dependent on a strong synergy between Cu and ZnO. Behrens et al. [14] pointed out that the integration of single Zn atoms into the copper surface enhances the catalyst activity and that the formation of a Cu/Zn surface alloy is an open discussed topic in methanol synthesis catalysts [15, 16]. On the other hand Kuld et al. [5] concluded from their results that the formation of this surface alloy leads to a strong decrease in H_2 binding energy on the copper surface which prohibits the probing of this surface with the common H_2-TPD technique. An analysis of the H_2-TPD desorption signal on Cu/Al_2O_3 and Cu/ZnO by Wilmer et al. [6], however, demonstrated that the desorption signal is shifted to higher temperatures in case of Cu/ZnO systems, i.e. the hydrogen is bond even stronger to the remaining copper surfaces in close contact with ZnO. Although the alumina present in these catalysts is commonly assumed to be only an irreducible structural support, Behrens et al. [17] recently showed that the incorporation of Al^{3+} into the ZnO framework has a significant effect on the $Cu/ZnO/Al_2O_3$ catalyst activity and has to be considered carefully in systematic catalyst development. With respect to these recent results it seems necessary to also explore the possible influence of alumina on the hydrogen adsorption on copper: Therefore, we present a systematic H_2-TPD study on polycrystalline copper and alumina supported copper to elucidate this issue.

Table 1 Summary of the characterization results of C and CA

	Cu/Al (mol %)	$n_{H2\text{-}TPD}$ (μmol g_{cat}^{-1})	$n_{N2O\text{-}RFC}$ (μmol g_{cat}^{-1})	S_{BET}^{a} (m^2 g_{cat}^{-1})
C	100/-	23.2 ± 0.5	33.5 ± 0.1	15/3.1
CA	84/16	89.3 ± 1.8	131.5 ± 2.1	46.6/n.d.

[a] Calcined sample/activated sample

2 Experimental and Computational Methods

2.1 Catalyst Preparation

The synthesis procedure of the polycrystalline copper catalyst C and the Cu/Al_2O_3 catalyst CA with the nominal Cu/Al_2O_3 ratio of 85/15 mol % is based on a co-precipitation concept for the industrial $Cu/ZnO/Al_2O_3$ catalyst, which has been recently reviewed in detail elsewhere [18]. The catalysts C and CA are precipitated from the metal nitrate solutions at a constant pH of 7 and a temperature of 303 K using a sodium carbonate solution as precipitating agent. After an aging period of 60 min the precipitate is filtered off, washed three times with bidestillated water, and dried at 80 °C over night. The dry powder is then calcined for 10 h at 593 K in $Q = 50$ sccm g^{-1} of synthetic air.

The metal content of the calcined precursors is analyzed by ICP-OES (SpectroFlame FTMOA81A, Spectro Analytical Instruments). Here, the samples are also checked for the absence of sodium and potassium impurities. Prior to the analysis, the samples are dissolved in boiling *aqua regia*, inspissated and diluted with 1 M HNO_3. Nitrogen physisorption of the calcined precursors is measured in a NOVA 4000e Surface Area & Pore Size Analyzer (Quantachrome Instruments) at 78 K. Prior to analysis, all samples are outgassed under vacuum at 523 K for 3 h. For analysis of the BET surface area ten evenly spaced points in the pressure region from 0.05 to 0.3 bar are used. The BET surface area of the reduced polycrystalline copper sample C is analyzed after the activation procedure (see below) in an Autosorb C (Quantachrome Instruments). A summary of the characterization parameters is presented in Table 1.

The copper surface area according to H_2-TPD and nitrous oxide reactive frontal chromatography (N_2O-RFC) are determined in a glass lined single-pass fixed-bed reactor (internal diameter 4.5 mm) with internal thermocouple, an upstream gas mixing unit and a mass spectrometer (Pfeiffer Vacuum OmniStar GSD 301 O) for time resolved in situ analysis, which is calibrated prior to every measurement. A detailed description and schematic representation of the setup is given in the supporting information. The system can be pressurized up to 28 bar and operated in a temperature range from 77 up to 773 K. During the catalyst activation, N_2O-RFC and H_2-TPD

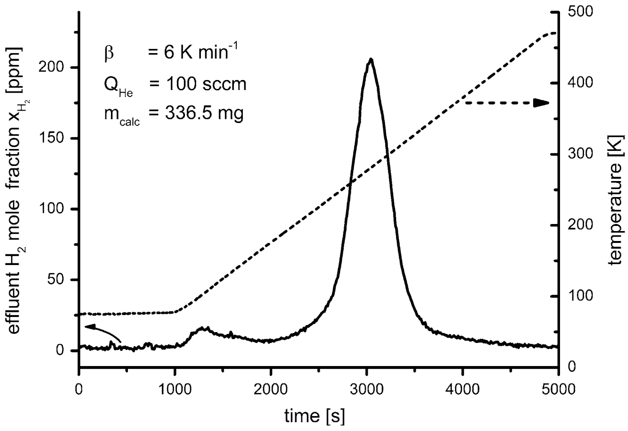

Fig. 1 Exemplary H_2-TPD of the polycrystalline copper sample C

measurements each catalyst is treated with the same gases of the following compositions and purities: H_2 (99.9999 %), He (99.9999), 2 % H_2 (99.9999 %)/He (99.9999), and 1 % N_2O (99.9990 %)/He (99.9999 %).

In a typical measurement $m_{calc} = 75$ mg (CA) or 350 mg (C) calcined catalyst of the 250–355 µm catalyst sieve fraction and 500 mg purified silicon carbide of the same sieve fraction are heated up at atmospheric pressure for 15 h in a mixture containing 2.0 % H_2 in He using the following temperature program: The temperature is raised from 300 to 448 K at 1 K min^{-1}, followed by switching to pure H_2 raising the temperature from 448 to 513 K at 1 K min^{-1} and holding for 30 min. For the activation procedure, a specific flow rate of 0.2 sccm g_{calc}^{-1} is used.

2.2 Hydrogen Temperature Programmed Desorption (H_2-TPD)

The H_2-TPD measurements follow a well established method described in Ref. [1]. The activated catalyst is cooled down to 235 K in helium and pressurized with 24 bar hydrogen for 30 min. A variation of the adsorption pressure and time showed that under these conditions full hydrogen coverage of copper is achieved. The catalyst is rapidly cooled down to 77 K, depressurized to atmospheric pressure and flushed at least 30 min with 100 sccm helium until the baseline in the mass spectrometer shows a constant value. Subsequently the catalyst bed is heated up under atmospheric pressure in a flow of Q = 100 sccm helium ramping linearly at β = 2, 4, 6 or 10 K min^{-1}. The desorption signal upon heating the catalyst bed is monitored in the mass spectrometer. A typical H_2-TPD curve is presented in Fig. 1. The symmetric H_2 desorption signal of copper is centered around ~280 K, very distinctive, and resembles single crystal UHV experiments by Anger et al. [7]. The amount of adsorbed hydrogen is calculated using the full area under the desorption peak. Apart from this desorption peak, a smaller one is found at ~90 K, which can be assigned to the desorption of weakly adsorbed hydrogen and nitrogen. In all cases, no significant signal above 350 K is visible, which stems from the decomposition of adsorbed water [19]. The raw data are corrected by subtracting a constant baseline. In order to account for possible sintering of the unsupported copper catalyst, every experiment is performed with a fresh activated amount of catalyst.

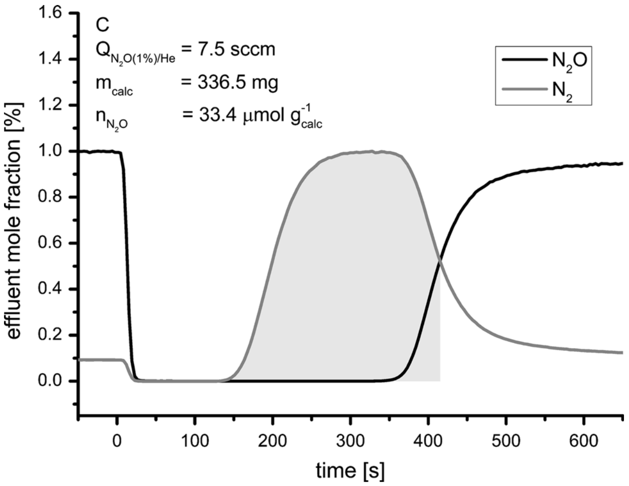

Fig. 2 Exemplary reactive N_2O frontal chromatography on polycrystalline copper. The area shaded in *gray* is used to determine the copper surface area

2.3 Reactive N_2O Frontal Chromatography

The N_2O copper surface area is determined at 1 bar pressure subsequent to the H_2-TPD experiment followed by cooling down to 308 K in helium. At this temperature, no significant bulk oxidation of copper is present and the N_2O decomposes on the copper surface following the reaction [1]:

$$N_2O + 2\, Cu_{\mathrm{surface}} \rightarrow Cu_2O + N_2$$

Holding the reactor under helium, the remaining setup is flushed with N_2O/He and after switching the reactor to 1 % N_2O/He a breakthrough curve in the reactor effluent stream is measured in the mass spectrometer. The amount of copper surface atoms is calculated from the catalyst mass, exact flow rate and N_2 area until the N_2O breakthrough. In order to determine the copper surface area, a mean copper surface atom density of 1.47×10^{19} atoms per m^2 is used. The latter one is the arithmetic mean value of the low index planes Cu(111), Cu(110), and Cu(100). As subsurface oxidation cannot be completely avoided, the intersection between the falling N_2 signal and rising N_2O signal at the breakthrough point is used as a limit for the integration of the N_2 signal. This is illustrated in Fig. 2.

Table 2 Facet distribution according to the Wulff construction and copper surface atom density per facet

	Cu (111)	Cu (110)	Cu(100)
η_{hkl} (%)	61	13	26
σ_{hkl} (mol m^{-2})	2.94×10^{-5}	1.79×10^{-5}	2.54×10^{-5}

2.4 Modelling of the Desorption Signal

In order to enable a well-founded comparison of the desorption processes on polycrystalline copper with Al_2O_3-supported systems, a mathematical model describing the desorption signals is used. The modelling approach to describe TPD flow experiments is well established has been extensively described in previous publications [20, 21]. In the most simple case (model 1), the desorption process is described by a second order process from a Cu(111) surface [21]. A coverage-dependent activation energy of desorption $(E_A - E_\Theta \Theta^n)$ is used to account for signal asymmetry and peak broadening. The resulting rate constant is implemented in an Arrhenius-type format:

$$k_{des} = k_{0,des} \times e^{-\frac{E_A - E_\Theta \Theta_H^n}{RT}}$$

Although, the theoretical distribution and different desorption behavior of the low-index (100), (110), and (111) copper facets is well known, this concept has not yet been applied for ZnO free systems [8, 9, 11, 22]. However, due to the absence of possible metal support interactions, the polycrystalline copper catalyst C is an ideal model system to validate this concept. Hence, in the second model (model 2) the presence of the three copper facets with a fixed ratio according to the Wulff construction is considered. In order to reduce the amount of model parameters, a common prefactor $k_{0,des} = 3.75 \times 10^{10} s^{-1}$, which has been derived from studies on $Cu/ZnO/Al_2O_3$ systems [21], and in case of model 2 also a facet independent, linear coverage-dependent activation energy is employed.

$$k_{des,hkl} = k_{0,des} \times e^{-\frac{E_{A,hkl} - E_\Theta \Theta_{H,hkl}}{RT}}$$

The facet distribution for crystalline copper is calculated using the software package WinXMorph [23, 24] and surface free energies for copper crystals in vacuum. [25]. The resulting facet distribution η_{hkl} and the copper surface atom density σ_{hkl} per facet are given in Table 2. These values are also in good agreement for H_2 treated copper particles adsorbed on ZnO [8].

The catalyst bed is described by a pseudo homogeneous continuous stirred tank reactor (CSTR) in absence of intraparticle mass transfer and H_2 readsorption on the catalyst surface. In prior studies, both processes showed to have no influence on the results under the given experimental conditions [21]. The governing equations are given as:

$$\frac{\partial n_{H_2}}{\partial t} = \dot{n}_{H_2,0} - \dot{n}_{H_2} - \sum N_{H_2,hkl} \frac{\partial \Theta_{\mathrm{H,hkl}}}{\partial t}$$

$$\frac{\partial \Theta_{\mathrm{H,hkl}}}{\partial t} = -2 k_{des,hkl} \Theta_{H,hkl}^2$$

Although, every facet exhibits a different surface structure, the Cu:H_2 adsorption stoichiometry is considered constant. Hence, the specific amount of adsorbed hydrogen N_{H_2} is a function of the respective copper surface atom density and the facet distribution:

$$N_{H_2} = \sum N_{H_2,hkl}$$

$$N_{H_2,100} : N_{H_2,110} : N_{H_2,111} = \eta_{100}\sigma_{100} : \eta_{110}\sigma_{110} : \eta_{111}\sigma_{111}$$

Solving the differential equations and the model parameter estimation is done in the Athena Visual Studio engineering software [26]. The hydrogen effluent mole fraction relative to the peak maximum value is chosen as objective function, gradients are calculated using a forward difference scheme, and the absolute objective function tolerance is set to 10^{-10}. For the parameter estimation the integrated Bayesian Estimation method is used.

The quality of the fit is evaluated using a dimensionless scaled root mean square error (SRMSE) between the experimental hydrogen effluent mole fraction x_{H_2} and the modelling result.

$$SRMSE = \frac{1}{X_{Ref}} \sqrt{\frac{1}{N} \sum_{j=1}^{N} \left(x_{H_2,experimental}(T_j) - x_{H_2,model}(T_j) \right)^2}$$

For the reference value X_{ref}, the experimental hydrogen effluent mole fraction at the peak maximum is used. For all peaks, the temperature region for determining the SRMSE values is between 225 K and 350 K. Reproduction experiments showed, that the SRMSE value of two desorption spectra with equal experimental conditions is roughly 0.04, which is a common value for flow TPD experiments [20].

3 Results and Discussion

The H_2-TPD results of the heating rate variation for C and CA and the corresponding SRMSE values for the parameterized models 1 and 2 are summarized in Table 3. An exemplary comparison of the H_2-TPD signals on the polycrystalline copper sample C with measurements on supported copper CA and modelling results according to model 1 is presented in Fig. 3.

Typically, the presence of strong metal support interaction alters the electronic properties of the metal surface and hence the adsorption properties [27, 28]. In case of

Table 3 Summary of the measurement and fitting results

Catalyst	N_{H2} (μmol g_{calc}^{-1})	N_{N2O} (μmol g_{calc}^{-1})	β (K min^{-1})	T^{a}_{max} (K)	SRMSE model 1	SRMSE^{b} model 2
C	22.7	n.d.	2	273	0.046	0.042/0.032
	23.2	n.d.	4	278	0.059	0.064/0.058
	23.0	33.6	6	282	0.042	0.051/0.043
	23.9	33.4	10	288	0.040	0.061/0.037
CA	87.2	n.d.	4	279	0.029	0.049/0.046
	90.3	130	6	284	0.032	0.064/0.045
	90.3	133	10	288	0.029	0.079/0.041

[a] From experimental curve

[b] Without coverage-dependency/with coverage-dependency

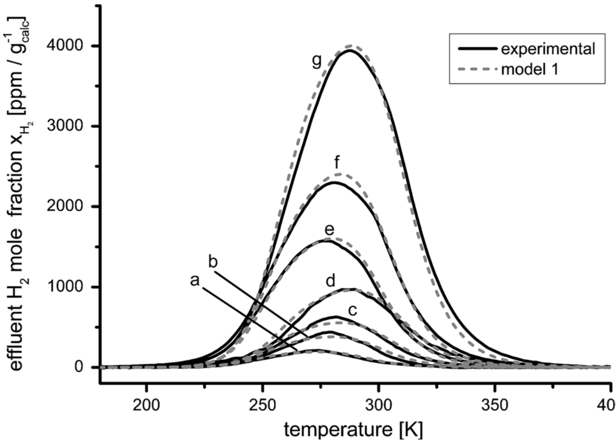

Fig. 3 Comparison of the experimental H_2-TPD *curve* with the parameterized model 1 for polycrystalline copper C (**a–d** β = 2–10 K min^{-1}) and for CA (**e–g**: β = 4–10 K min^{-1})

Table 4 Optimized parameters for model 1 and 2

Model 1	Model 2
$E_A = 71.26 \pm 0.11$ kJ mol^{-1}	$E_{A,100} = 63.97 \pm 0.14$ kJ mol^{-1}
$E_\Theta = 5.27 \pm 0.11$ kJ mol^{-1}	$E_{A,110} = 78.46 \pm 0.54$ kJ mol^{-1}
$n = 2.33 \pm 0.11$	$E_{A,111} = 71.01 \pm 0.16$ kJ mol^{-1}
	$E_\Theta = 0.98 \pm 0.2$ kJ mol^{-1}

In both models a fixed prefactor of $k_{0,des} = 3.75 \times 10^{10}\ s^{-1}$ is used

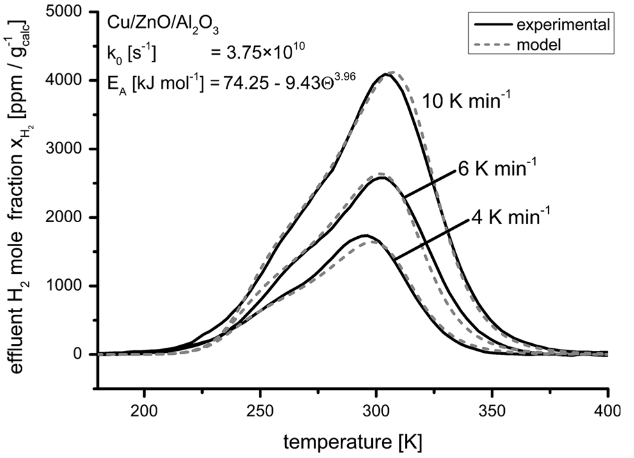

Fig. 4 Modelling results of H_2-TPD spectra from a $Cu/ZnO/Al_2O_3$ catalyst

Cu/ZnO systems the formation of partially amorphous ZnO_x overlayers and thin polar ZnO films is observed and the effect of partial alloying of Zn atoms into the copper surface on methanol synthesis has been studied in detail. [14, 29] It also leads to a shift of the desorption maximum to higher temperatures. The peak maximum temperatures of CA very much resemble the ones of the polycrystalline copper sample C and are in good agreement with literature data for other Cu/Al_2O_3 systems [6]. This suggests that Al_2O_3 in fact only acts a rigid support for the copper particles and has no pronounced influence on the electronic structure of the system.

This is also supported by the high similarity of the peak shapes of C and CA. Although the specific copper surface area of CA results in a roughly four times higher value than of C, all signals can be described by the same model. The optimized parameters for the evaluated models 1 and 2 are presented in Table 4.

In both cases acceptable SRMSE values below or only slightly above 0.04 can be achieved. In model 1 the obtained parameters for the coverage dependency are very similar to values for $Cu/ZnO/Al_2O_3$ systems [21] and the roughly 15 K lower temperature onset of the desorption signal is accounted for by a slightly (4 kJ mol^{-1}) lower activation energy of desorption. It should be noted, that in this model the coverage dependence factor *n* defines the desorption signal asymmetry and has no real physical meaning. This can be nicely illustrated by applying model 1 on a highly asymmetric H_2-TPD spectrum: Fig. 4 shows the H_2-TPD spectrum and corresponding modelling result for a high performance $Cu/ZnO/Al_2O_3$ catalyst presented in Ref. [4]. Although the catalyst clearly exhibits an at least

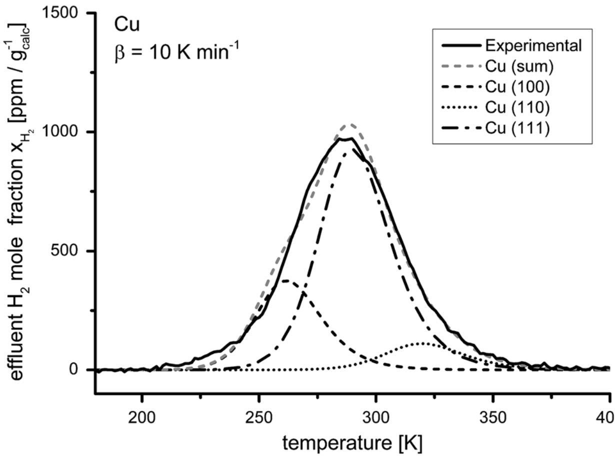

Fig. 5 Exemplary description of the desorption signal of H_2 from polycrystalline copper considering the presence of (111), (110) and (100) facets

bimodal desorption signal, is can be accurately described by a coverage-dependent desorption from one single copper facet.

A physically more reasonable interpretation of the desorption signal can be achieved by considering the presence of the low-index (100), (110), and (111) copper facets in model 2. An exemplary description of the desorption signal according to this model is presented in Fig. 5.

As mentioned above, the fixed facet distribution is deduced from a Wulff construction, which is only valid for free copper crystals. Although, the alumina support structure seems to have no significant electronic influence on the desorption process, it is not known a priori, whether other influences like a preferred contact orientation of the copper facets on alumina exists. Therefore, the fitting process is only applied on the polycrystalline copper sample C and the obtained model parameters are transferred without further alteration to the CA sample. Compared to model 1 this leads to slightly worse SRMSE values for CA, however, the overall model is still in good agreement with the measures spectra which confirms the statement that the alumina support has no significant influence on the exposed copper particle surface. The obtained activation energies result in a desorption process starting from Cu(100) followed by Cu(111) and ending with Cu(110). The same order has been observed and discussed for desorption in differently pretreated $Cu/ZnO/Al_2O_3$ systems [22]. In order to estimate the coverage dependency of the desorption process, the model is also parameterized without a coverage dependent activation energy of desorption E_Θ (see Table 3). It turns out that the introduction of a linear adsorbate dependency of roughly $E_\Theta = 1$ kJ mol^{-1} significantly enhances the description of the experiments and should not be omitted. It should be noted that this model has to be considered very carefully when applying it to describe the facet distribution in coprecipitated $Cu/ZnO/Al_2O_3$ catalysts. In contrast to catalysts presented e.g. in Ref. [8] and [9], the system in Fig. 4 is not considered a standard metal-support system with (faceted) copper nanoparticles sitting on top of a bulk ZnO support, but rather a porous aggregate of quasi-spherical ZnO and Cu nanoparticles of equal size (see Ref. [4]). Furthermore, parts of the copper spheres are covered with a partially reduced ZnO_x layer. Due to the complex three dimensional structure, with multiple different Cu–ZnO interfaces per particle, the description of such systems with the Wulff construction has to be examined very carefully. However, as Kuld et al. [5] recently showed, the oxidation state of the ZnO in $Cu/ZnO/Al_2O_3$ catalysts can be influenced by the activation procedure and subsequently analyzed via H_2-TPD and N_2O-RFC. In combination with a shape analysis of the H_2 desorption signal this could be used to systematically control and analyze the extent of the SMSI effect in such heterogeneous systems and its influence on the signal shape.

In all experiments, the ratio of consumed N_2O to adsorbed H_2 is roughly 1.45, which corresponds with a $Cu:H_2$ adsorption stoichiometry of 2.9. This is in line with an atomic hydrogen saturation coverage of $^2/_3$ ML ($Cu:H_2 = 3$). Although, classically a coverage of $^1/_2$ ML is deduced from UHV studies, the formation of a $^2/_3$ ML coverage has been observed under higher adsorption pressures [30, 31]. Furthermore, it has recently been shown [4, 5] that the commonly assumed adsorption stoichiometry of $Cu:H_2 = 4$ in $Cu/ZnO/Al_2O_3$ catalysts suffers from an overestimation of the copper surface area by N_2O-experiments. Assuming a saturation H-coverage of $^2/_3$ ML and a mean copper surface atom density of 1.47 10^{19} m^{-2}, the mean surface area of the polycrystalline copper sample C is 2.9 m^2 g_{calc}^{-1}. This is in excellent agreement with the BET surface area of the activated sample C (3.1 m^2 g_{calc}^{-1}) and underlines the high sensitivity achievable with H_2-TPD.

4 Conclusion

The exposed copper surface area of polycrystalline copper and a Cu/Al_2O_3 system was successfully characterized with hydrogen temperature programmed desorption. A comparison of the obtained signals points out that the alumina support has no significant influence on the desorption signal and that both systems can be described using the same mathematical models. It can be concluded from the results that the shift of the desorption maximum in $Cu/ZnO/Al_2O_3$ catalysts to higher temperatures is indeed a function of the Cu/ZnO synergy and is not directly correlated to a

Cu/Al_2O_3 interaction. Furthermore, it was demonstrated that the desorption signal can be accurately described using a theoretically derived distribution of the low-index (100), (110) and (111) facets according to the Wulff construction for free copper crystals. Within the scope of copper based $Cu/ZnO/Al_2O_3$ methanol synthesis catalyst these experiments strengthen our understanding of the catalytic activity, which is determined by metal support interaction and by mutual influence of the specific catalyst components.

Acknowledgments Matthias Fichtl gratefully acknowledges the support of the TUM Graduate School. The authors thank Prof. Martin Muhler, Prof. Robert Schlögel, Prof. Malte Behrens, Dr. Nikolas Jacobsen, Dr. Wilma Busser, and Julia Schumann for fruitful discussions.

References

1. Hinrichsen O, Genger T, Muhler M (2000) Chem Eng Technol 23:956–959
2. Chinchen GC, Hay CM, Vandervell HD, Waugh KC (1987) J Catal 103:79–86
3. Kurtz M, Bauer N, Büscher C, Wilmer H, Hinrichsen O, Becker R, Rabe S, Merz K, Driess M, Fischer RA, Muhler M (2004) Catal Lett 92:49–52
4. Fichtl MB, Schumann J, Kasatkin I, Jacobsen N, Behrens M, Schlögl R, Muhler M, Hinrichsen O (2014) Angew Chem Int Ed. doi:10.1002/ange.201400575
5. Kuld S, Conradsen C, Moses PG, Chorkendorff I, Sehested J (2014) Angew Chem Int Ed 53:5941–5945
6. Wilmer H, Genger T, Hinrichsen O (2003) J Catal 215:188–198
7. Anger G, Winkler A, Rendulic KD (1989) Surf Sci 220:1–17
8. Hansen PL, Wagner JB, Helveg S, Rostrup-Nielsen JR, Clausen BS, Topsøe H (2002) Science 295:2053–2055
9. Grunwaldt J-D, Molenbroek A, Topsøe N-Y, Topsøe H, Clausen BS (2000) J Catal 194:452–460
10. Wilmer H, Hinrichsen O (2002) Catal Lett 82:117–122
11. Ovesen CV, Clausen BS, Schiøtz J, Stoltze P, Topsøe H, Nørskov JK (1997) J Catal 168:133–142
12. Peter M, Fichtl MB, Ruland H, Kaluza S, Muhler M, Hinrichsen O (2012) Chem Eng J 203:480–491
13. Vesborg PCK, Chorkendorff I, Knudsen I, Balmes O, Nerlov J, Molenbroek AM, Clausen BS, Helveg S (2009) J Catal 262:65–72
14. Behrens M, Studt F, Kasatkin I, Kühl S, Hävecker M, Abild-Pedersen F, Zander S, Girgsdies F, Kurr P, Kniep B-L, Tovar M, Fischer RW, Nørskov JK, Schlögl R (2012) Science 336:893–897
15. Fujitani T, Nakamura J (2000) Appl Catal A 191:111–129
16. Sano M, Adaniya T, Fujitani T, Nakamura J (2002) J Phys Chem B 106:7627–7633
17. Behrens M, Zander S, Kurr P, Jacobsen N, Senker J, Koch G, Ressler T, Fischer RW, Schlögl R (2013) J Am Chem Soc 135:6061–6068
18. Behrens M, Schlögl R (2013) Z Anorg Allg Chem 639:2683–2695
19. Hinrichsen O, Genger T, Muhler M (2000) In: Corma A, Melo FV, Mendioroz S, Fierro JLG (eds) Studies in Surface Science and Catalysis. Elsevier,Amsterdam, pp 3825–3830
20. Kanervo JM, Keskitalo TJ, Slioor RI, Krause AOI (2006) J Catal 238:382–393
21. Peter M, Fendt J, Wilmer H, Hinrichsen O (2012) Catal Lett 142:547–556
22. Peter M, Fendt J, Pleintinger S, Hinrichsen O (2012) Catal Sci Technol 2:2249
23. Kaminsky W (2007) J Appl Crystallogr 40:382–385
24. Kaminsky W (2005) J Appl Crystallogr 38:566–567
25. Vitos L, Ruban AV, Skriver HL, Kollár J (1998) Surf Sci 411:186–202
26. Athena Visual Studio, Version 14.2, www.athenavisual.com
27. Campbell CT (2012) Nat Chem 4:597–598
28. Herrmann JM (1984) J Catal 89:404–412
29. Schott V, Oberhofer H, Birkner A, Xu M, Wang Y, Muhler M, Reuter K, Wöll C (2013) Angew Chem Int Ed 52:11925–11929
30. Lee G, Poker DB, Zehner DM, Plummer EW (1996) Surf Sci 357–358:717–720
31. Mccash EM, Parker SF, Pritchard J, Chesters MA (1989) Surf Sci 215:363–377